JOURNAL OF SOLID STATE CHEMISTRY 120, 105–111 (1995)

Electrical Transport Properties and High-Temperature Thermoelectric Performance of $(Ca_{0.9}M_{0.1})MnO_3$ (M = Y, La, Ce, Sm, In, Sn, Sb, Pb, Bi)

Michitaka Ohtaki,[1] Hisako Koga, Tsutomu Tokunaga, Koichi Eguchi, and Hiromichi Arai

Department of Materials Science and Technology, Graduate School of Engineering Sciences, Kyushu University, 6-1 Kasugakoen, Kasuga-shi, Fukuoka 816, Japan

Received March 13, 1995; revised July 19, 1995; accepted July 26, 1995

The electrical transport properties of $(Ca_{0.9}M_{0.1})MnO_3$(M = Y, La, Ce, Sm, In, Sn, Sb, Pb, Bi) are investigated in terms of a new material for high-temperature thermoelectric conversion. The substitution at the Ca site causes a marked increase in the electrical conductivity σ, along with a moderate decrease in the absolute value of the Seebeck coefficient S. The plots of log σT vs $1/T$ show a negative linear relation, indicating that hopping conduction occurs in these oxides. The σ values at room temperature increase with increasing ionic radii of the cation substituents, implying an increase in the carrier mobility due to larger intersite distance for hopping. The sample of $(Ca_{0.9}Bi_{0.1})MnO_3$ attains the largest power factor, 2.8×10^{-4}/W m^{-1}K^{-2}, at 800°C and leads to the figure of merit 0.7–0.75 $\times$ 10^{-4}K^{-1} over the wide range of temperatures 600–900°C. The oxide shows a maximum ZT value of 0.085 at 900°C.

INTRODUCTION

Thermoelectric power generation utilizes the Seebeck effect in solid materials to convert thermal energy directly to electrical energy (1). Three fundamental physical parameters related to the electrical and thermal transport properties of solids, the electrical conductivity σ, the Seebeck coefficient S, and the thermal conductivity κ, govern the conversion efficiency of thermoelectric devices. The figure of merit for thermoelectric conversion, defined by $Z = S^2\sigma/\kappa$, is a primary criterion for the thermoelectric materials constituting the devices. Because these three parameters are all closely connected with the scattering mechanisms of charge carriers and lattice vibrations (phonons), they are dependent upon each other, and optimization of the thermoelectric performance always requires a compromise between them. Moreover, theories of conventional broad-band semiconductors predict that there is a general tendency for S and σ to vary in a reciprocal way. These facts cause serious problems in development of thermoelectric materials and hence in practical utilization of thermoelectric power generation. Some semiconducting materials are reported to have unexpectedly promising thermoelectric properties, much better than predicted by the broad-band theories for which the free electron approximation holds good. These materials include transition metal disilicides and boron carbides, in which hopping conduction occurs (2, 3). Development of new materials, however, is still the most important issue for practical application of thermoelectric power generation.

Since the Carnot efficiency, η_c, of the thermoelectric system improves with increasing temperature difference, high-temperature operation is an alternative route to improving the conversion efficiency. A higher operating temperature, T, yields a larger dimensionless figure of merit, ZT, which has a value near one or higher in efficient materials. High durability at elevated temperatures is therefore essential for thermoelectric materials to attain highly efficient energy conversion. As high-temperature thermoelectric materials, Si–Ge alloys (4–6), several metal chalcogenides (7, 8), transition metal disilicides (9–11), and some boron compounds (12–14) have been of much interest. However, besides the difficulties and high costs of fabricating devices with these materials, they generally have inevitable shortcomings for practical use at high temperature in ambient air. Many of them require costly surface protection to prevent vaporization or surface oxidation, and some others have an inherent limitation in high-temperature operation due to phase transitions at high temperatures.

In terms of heat resistance, oxide materials are apparently advantageous, since most metal oxides in their common oxidation states are highly stable at elevated temperature in air. Nevertheless, research on oxide thermoelectric materials has scarcely been reported, although there are a large number of publications on electrical conduction and the Seebeck effect in metal oxides. The major reason

[1] To whom correspondence should be addressed.

0022-4596/95 $12.00

for such lack of enthusiasm for research on oxide thermoelectric materials appears to be the rather low values of the carrier mobilities often observed for many oxide semiconductors, which are thought to be due to the highly ionic character of oxides. Some metal oxides, however, exhibit rather high carrier mobility. Fonstad *et al.* reported that an SnO_2 single crystal showed a Hall carrier mobility of 150–260 cm^2/V sec at 300 K (15). These values are much higher than the 30 cm^2/V sec reported for metallic ReO_3 (16). We have already pointed out that some mixed metal oxides based on In_2O_3, which is also well known as a highly conductive oxide, exhibited high thermoelectric performance, and that they would be promising as new candidate materials for high-temperature thermoelectrics (17). Moreover, sintered bodies of these oxides can be prepared easily by conventional ceramic processes in ambient air and are apparently stable in air at least up to 1400°C without any surface protection.

Perovskite-type oxides form a large family of metal oxides, since many kinds of metal elements can fit into the perovskite structure. The electronic properties of these oxides also range widely from collective to localized electrons (18), and several perovskite-type oxides are well known as highly conductive ceramics. Although there have been an enormous number of studies on the electrical, as well as the magnetic, properties of the perovskite-type oxides, those focused on applicability as thermoelectric materials are very scarce. Bates *et al.* examined the electrical and thermal transport properties of (Y, Ca)CrO_3 and (La, Sr) CrO_3 and reported their ZT values as 0.03–0.09 at 1000°C (19); these chromites have poor sinterability, which also causes serious problems in their application to solid oxide fuel cells. A few high-temperature superconducting cuprates having perovskite-related structures were once proposed as low-temperature materials for thermoelectric cooling (20), but the proposal was concluded to be hopeless because of their very low carrier mobility due to the highly localized nature of these cuprates (21, 22). Kobayashi *et al.* (23) recently reported that the substitution of some lanthanide elements for Ca in $CaMnO_3$ raised the electrical resistivity below room temperature, resulting in an increase of the semiconductor-to-metal transition temperature. Although they also suggested the possibility of the oxides as thermoelectric materials, the focus of their investigation was neither on the increased conductivity in the hopping conduction regime above the transition temperature nor on the thermoelectric performance at high temperatures. On $CaMnO_3$ and related materials, there have been many reports on electrical and magnetic properties, but most of them dealt with the properties at room temperature or below (24–27). We have hence started our studies on the thermoelectric properties of partially substituted perovskite-type oxides with respect to high-temperature thermoelectric applications. This paper describes the effects of substitution at the Ca site of $CaMnO_3$ on its electrical transport properties with a focus on thermoelectric performance at high temperature. The thermal conductivity and the figure of merit of the materials are also discussed.

EXPERIMENTAL

All samples of the $CaMnO_3$-based mixed oxides were prepared by solid state reaction from fine powders of $CaCO_3$, $MnCO_3$, and single oxides of metal substituents. All the raw materials were of guaranteed grade (>99.9%) and were used without further purification. These powders were kept in a drying oven at about 100°C and then cooled in a desiccator before weighing. Powders of two carbonates and a metal oxide as a substituent were weighed at a nominal proportion, mixed in a nylon-lined ball mill for 24 hr, and calcined at 850°C for 10 hr in air. The mixture was then pulverized with an alumina mortar and uniaxially pressed into a pellet. The pellet was sintered at 1300°C for 10 hr in air.

The electrical measurements were carried out on specimens cut from the sintered pellets as parallelepiped bars of ca. $4 \times 3 \times 15$ mm in size and polished with SiC emery papers. The electrical conductivity σ and the Seebeck coefficient S were measured simultaneously at the steady-state temperature. The mesurement procedures and an experimental setup have been described elsewhere in detail (17). Briefly, two 13%Rh/Pt–Pt thermocouples were attached on both end surfaces of the sample bar, and another two Pt paste electrodes were placed between them in the standard four-wire arrangement. First, after an even and steady temperature was attained, σ was measured by the dc four-wire technique using Pt legs of each Pt/Rh–Pt thermocouple as current leads. Subsequently, small (<5 K) and steady-state temperature gradients of varying extent were applied by a heater located near one end of the sample, and then S was obtained from the slope of the least-square regressions of the thermoelectromotive force as a function of the temperature difference. The measurements were carried out from room temperature up to 1000°. Crystal phases in the samples were examined by a powder X-ray diffraction (XRD) study. The relative density of the sintered samples was determined by Archimedes' method. The thermal conductivity κ was determined from the thermal diffusivity and the specific heat capacity measured by the laser flash technique on an ULVAC TC-7000 thermal constant measurement sytem. The measurements were carried out for sample disks ca. 10 mm in diameter and 1–2 mm in thickness at up to 1000°C *in vacuo*. All the κ measurements were calibrated with a standard sample of sapphire single crystal.

RESULTS AND DISCUSSION

The Electrical Conductivity

The Ca site of $CaMnO_3$, usually referred as the A site of ABO_3 perovskite-type oxides, was subjected to partial

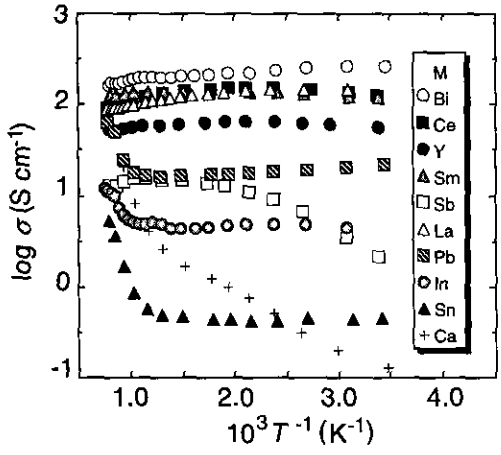

FIG. 1. The temperature dependence of the electrical conductivities for $(Ca_{0.9}M_{0.1})MnO_3$.

substitution by tri- or tetravalent metal cations of lanthanide-related elements Y, La, Ce, and Sm, and later typical elements In, Sn, Sb, Pb, and Bi. All samples obtained here were apparently dense sintered bodies with more than 95% of theoretical density. An XRD study confirmed that all the substituted oxides at least up to 10 at.% substitution consist of a single phase having the $CaMnO_3$ crystal structure and detected no impurity phases containing the metal substituents. The XRD patterns of all the samples exhibited strong diffraction lines assigned to $CaMnO_3$ in cubic symmetry and also showed some very weak lines which can be ascribed to an oxygen-deficient perovskite phase with defect ordering, $Ca_2Mn_2O_5$, in which Mn ions are trivalent. These results are consistent with previous reports which mentioned that in $CaMnO_3$ fired at 1350–1400°C in air, only 80% of Mn ions were tetravalent (24, 25). Whereas the exact valency and spin-state of the Mn ion and the oxygen content of the samples have not yet been determined, X-ray photoelectron spectroscopy confirmed that the Mn $2p3/2$ spectra of both doped and undoped samples gave virtually the same peak position, 642.3 eV, using the Au $4f7/2$ spectrum as a standard, and that this peak position corresponds to that of MnO_2. We therefore assumed that Mn^{4+} is the dominant manganese species in our samples, and the difference in the oxygen deficiency is negligible.

The effects of the substitution on the electrical conductivity of $(Ca_{0.9}M_{0.1})MnO_3$ are summarized in Fig. 1. The oxide $CaMnO_3$ with no substitution was an n-type semiconductor having rather low values of σ, ca. 10^{-1} S/cm at room temperature, consistent with the values reported by McChesney *et al.* (27). Goodenough reported that $CaMnO_3$ is classified as a semiconducting oxide having a localized valence band and a collective conduction band (28). At room temperature, all the substituted samples showed σ values much higher than that of the undoped sample. Of particular interest is the Bi substitution, which resulted in an increase in σ by more than 3 orders of magnitude. Moreover, the temperature coefficients, $d\sigma/dT$, of the substituted samples changed from positive to nearly zero or negative, except that of the Sb-substituted one. Even for the Sb substitution, $d\sigma/dT$ decreases with increasing temperature and turns negative at around 600°C. The highest conductivity occurs for the Bi-substituted sample, which shows negative values of $d\sigma/dT$ within the whole temperature range examined.

The Conduction Mechanism

Negative values of $d\sigma/dT$ usually imply metallic conduction. However, hopping conduction with a small activation energy may also cause negative $d\sigma/dT$. For hopping conduction, in which hopping of the charge carriers is thermally activated with the activation energy E_a, the electrical conductivity σ is given as

$$\sigma = (C/T)\exp(-E_a/kT), \qquad [1]$$

where k is the Boltzmann constant (29). The equation predicts a linear relation between $\log \sigma T$ and $1/T$ instead of the usual Arrhenius plots for the electrical conductivity.

Figure 2 presents the plots of $\log \sigma T$ versus $1/T$ for $(Ca_{0.9}M_{0.1})MnO_3$. In the temperature region below 300°C, the plots for all the samples except the Sb-substituted one lie on the straight lines, confirming the applicability of Eq. [1]. Moreover, the highly conductive samples with Bi, La, Ce, Sm, or Y retain linearity at much higher temperatures, e.g., up to 500–800°C. This would be attributed to an extension of the extrinsic region due to the doping effect of tri- or tetravalent cations. The undoped $CaMnO_3$ gives a steeper straight line up to 400°C, yielding an activation

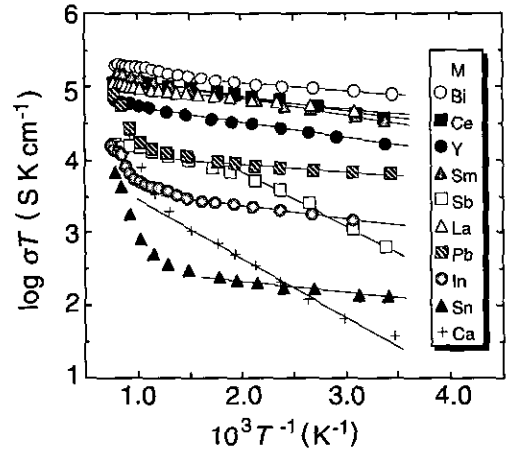

FIG. 2. The relation between $\log \sigma T$ of $(Ca_{0.9}M_{0.1})MnO_3$ and $1/T$.

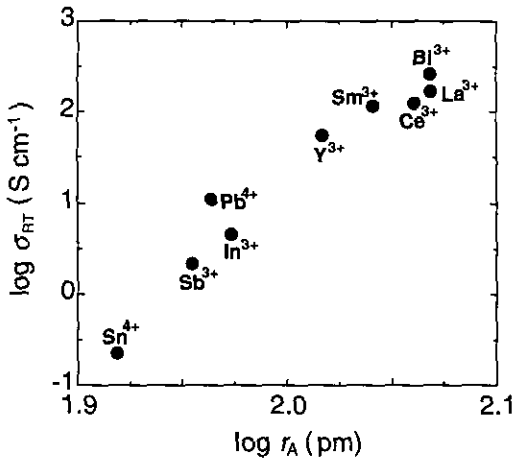

FIG. 3. The electrical conductivities of $(Ca_{0.9}M_{0.1})MnO_3$ at room temperature as a function of the ionic radii of the cation substituents M.

energy E_a of 0.16 eV. This value is in good agreement with the 0.192 eV reported for $LaCrO_3$ (29) and 0.19 ± 0.01 eV for $LaMnO_3$ (30). The plots for all the samples with substituents except Sb yield small and virtually equal values of E_a of 0.02–0.04 eV. For Sb substitution, the plots below 150°C appear to be on a straight line with E_a of ca. 0.16 eV, very similar to that of the undoped sample.

The linear relation seen in Fig. 2 implies a hopping conduction mechanism in the $CaMnO_3$-based oxides. The electrical conductivity of small polaron hopping in the adiabatic case, with the intersite distance a, can be written as

$$\sigma = ne\mu = nea^2(A/T)\exp(-E_h/kT), \qquad [2]$$

where n is the carrier concentration, e the electrical charge of the carrier, μ the carrier mobility, E_h the activation energy for hopping, and A the pre-exponential term related to the carrier scattering mechanism (31). If differences in n, A, and E_h between the samples are sufficiently small, Eq. [2] at a certain temperature can give rise to a linear relation between log σ and log a.

Figure 3 clearly depicts the surprisingly good linearity between the logarithm of ionic radii, r_A, of the cation substituents and the logarithm of the electrical conductivity at room temperature, σ_{RT}, for all the $CaMnO_3$-based oxides with the A-site substitution at 10 at.%. In this figure, the carrier concentrations n are assumed to be predominantly governed by the concentrations of the dopant cations. The σ_{RT} values for Pb^{4+} and Sn^{4+} in Fig. 3 are therefore adjusted by a factor of 0.5, because these tetravalent cations substituting on the divalent Ca sites can provide twice the number of carrier electrons than the trivalent cations. Undoped $CaMnO_3$ is completely inconsistent with the linearity in Fig. 3, having much lower σ. It should be noted that the ionic radii presented here are the values for 6-fold coordination, according to Shannon (32), since we cannot find a complete list of values for 12-coordination, which is actually the case for A-site cations in the perovskite-type oxides. Moreover, as mentioned above, the assumption of almost the same value of E_h may no longer hold, which is certainly so for the Sb-substituted sample. Nevertheless, in spite of the extreme simpleness of the estimation, Fig. 3 suggests that the hopping intersite distance, which presumably varies with the ionic radii of the cation substituents, mainly governs the condutivity at low and intermediate temperatures. This implies that the change in conductivity is due to an increase in the carrier mobility. These results indicate that a hopping conduction mechanism is highly probable for the $CaMnO_3$-based, partially substituted, perovskite-type oxides in the present study. Based on a reported value of the lattice constant of cubic $CaMnO_3$ as 7.465 Å (corresponding to an edge of 3.73 Å for the perovskite pseudocell) (24, 25, 27), the dopant concentration of 0.1 per formula unit, and the electrical conductivities at room temperature, the carrier mobilities can be calculated as 0.86 cm^2/V sec at the highest for the Bi-substituted sample, as well as 0.18 and 0.015 cm^2/V sec for the Y- and In-substituted ones, for instance. These values are consistent with the higher limit of the mobility predicted from the small polaron hopping mechanism, 1.0–0.1 cm^2/V sec. To elucidate the true nature of the conduction mechanism, however, further investigation will be necessary, e.g., exact carrier concentrations, the Hall mobility, the spin-state of the electrons, the activation energy of carrier generation and hopping, and the detailed crystal and defect structure of the samples as well.

The Seebeck Coefficient

The temperature dependence of the Seebeck coefficients, S, of the samples is summarized in Fig. 4. All samples

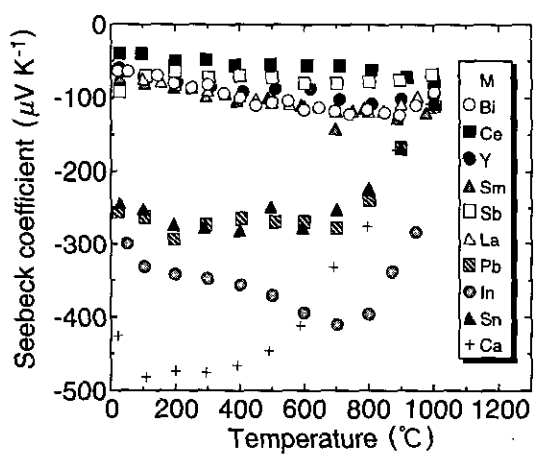

FIG. 4. The temperature dependence of the Seebeck coefficients for $(Ca_{0.9}M_{0.1})MnO_3$.

have negative values of S, indicating n-type conduction. The absolute values of S decrease with substitution at the Ca site in most cases. This tendency appears to be in fairly good agreement with the increase in σ with substitution, as seen in Fig. 1, and would be ascribed to an increase in the carrier concentrations. Even though the suppression of S as seen in Fig. 4 is apparent, the absolute values of S are still fairly large. Even for the highly conductive samples substituted by Bi, La, Sm, and Y, they retain S values of about $-80\ \mu V/K$ at room temperature. Moreover, it should be noted that the absolute value of S for these samples increases almost linearly with increasing temperature, at least up to 800°C, and attains a value of $-120\ \mu V/K$ for the Bi-substituted sample. Such absolute values of S are definitely too large for metallic conduction. Although the principles of small polaron hopping conduction predict an almost temperature-independent Seebeck coefficient (31), linear increase in Seebeck coefficients with increasing temperature has also been reported for polaron hopping conduction in $LaCrO_3$ (19) and hopping between inequivalent sites in boron carbides (12, 33, 34).

Thermoelectric Performance and Applicability to High Temperature Thermoelectric Materials

Since thermoelectric applications require high σ and large S, the thermoelectric properties of the perovskite-type oxides $(Ca_{0.9}M_{0.1})MnO_3$ described above are of great interest in high-temperature thermoelectrics. Their electrical conductivities are markedly high, and yet the absolute values of their Seebeck coefficients are fairly large, showing an almost linear increase with increasing temperature. Moreover, because the samples of these oxides are prepared by sintering at 1300°C in air, the oxides are considered to be stable at temperatures even higher than 1000°C in ambient air, accordingly. These facts strongly suggest that these oxides are promising for thermoelectric applications at high temperature.

The power factor $S^2\sigma$ evaluates the electrical components of the thermoelectric performance. The temperature dependence of the power factors of $(Ca_{0.9}M_{0.1})MnO_3$ calculated from the data in Figs. 1 and 4 is plotted in Fig. 5. Clearly, the Bi-substituted sample shows the largest power factor of all the samples. The power factor of the oxide increases up to 800–900°C and then rapidly decreases, attaining a maximum value of 2.8×10^{-4} W/m K^2. Although some other $CaMnO_3$-based oxides, such as those with Sm, La, and Pb dopants, also show rather good power factors, the results of the Bi-substituted sample are much superior.

The band theories for conventional semiconductors with broad-band electronic structure predict that higher carrier mobility leads to larger values of both the electrial conductivity and the Seebeck coefficients (35, 36). In Eq. [2], an increase in a, the mean distance between the hopping sites,

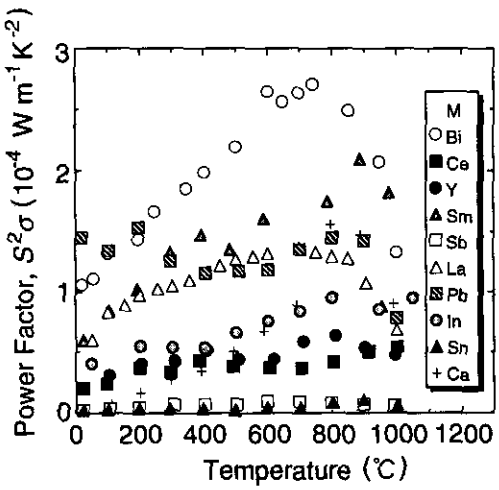

FIG. 5. The temperature dependence of the power factors for $(Ca_{0.9}M_{0.1})MnO_3$.

yields a higher mobility of the carriers. One can see that the larger cations such as Bi^{3+} and La^{3+} give larger power factors, whereas the smaller ones such as Sn^{4+} and Sb^{3+} result in marked depression of the thermoelectric performance. Although there are, of course, some exceptional cases, such as Ce^{3+} and In^{3+}, it would be reasonable to attribute the improved performance to an increase in mobility due to larger sizes of the substituent cations. We therefore further examined the most promising candidate, $(Ca_{0.9}Bi_{0.1})MnO_3$.

To maintain a temperature difference sufficient to generate large thermoelectromotive force, thermoelectric power generation requires that the thermal conductivity κ of the materials should be low. The κ value of $(Ca_{0.9}Bi_{0.1})MnO_3$ at room temperature was 3.0 W/mK, almost the same as that of undoped $CaMnO_3$. As shown in Fig. 6, however,

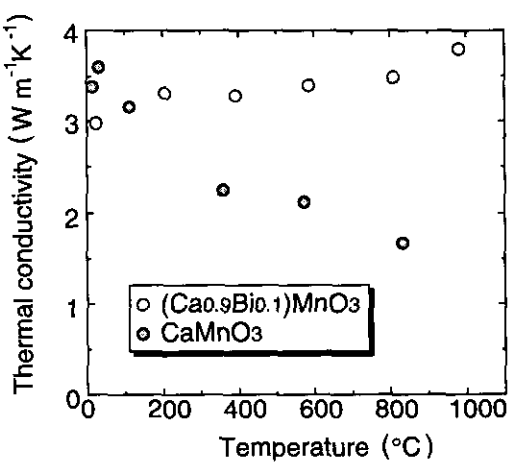

FIG. 6. The temperature dependence of the thermal conductivities for $(Ca_{0.9}Bi_{0.1})MnO_3$ and $CaMnO_3$.

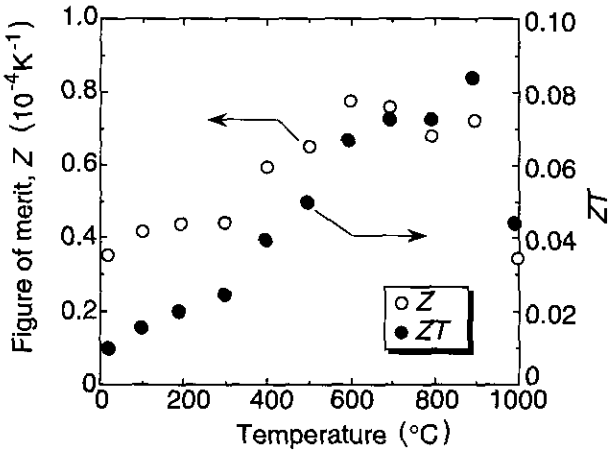

FIG. 7. The temperature dependence of the figures of merit Z and the dimensionless figures of merit ZT for $(Ca_{0.9}Bi_{0.1})MnO_3$.

the κ of $(Ca_{0.9}Bi_{0.1})MnO_3$ increased slighly with increasing temperature, whereas that of undoped $CaMnO_3$ decreased. Nevertheless, the κ of $(Ca_{0.9}Bi_{0.1})MnO_3$ does not exceed 3.8 W/mK even at 1000°C. The figure of merit, $Z = S^2\sigma/\kappa$, of $(Ca_{0.9}Bi_{0.1})MnO_3$ thereby attains values of 0.7–0.75 $\times$ 10^{-4} K^{-1} in the rather wide temperature range 600–900°C, and the maximum value of the dimensionless figure of merit, ZT, is 0.085 at 900°C (see Fig. 7). This value is slightly larger than those reported for (La, Sr)CrO_3 (19) at 900°C, and at lower temperatures the present ZT values are much larger than for (La, Sr)CrO_3. In addition, our samles have no problems with sinterability as the lanthanum chromites generally have, because the relative densities of the $CaMnO_3$-based oxides easily reach more than 95%.

The maximum Z values obtained here are about half those estimated for $(Ln_{0.1}Ca_{0.9})MnO_3$ (Ln = Y, Tb, Ho) by Kobayashi *et al.* In their estimation, however, the κ values of $LaCrO_3$ reported by Weber *et al.* (19) were used instead of the real values of their own samples. Because the electrical conductivities of $(Ln_{0.1}Ca_{0.9})MnO_3$ were about an order of magnitude higher than that of $La_{0.9}Sr_{0.1}CrO_3$ reported by Weber *et al.*, the actual values of κ of $(Ln_{0.1}Ca_{0.9})MnO_3$ would also be much higher than the values used in their estimation and would lead to the much lower Z in reality.

At present, the Z values of $(Ca_{0.9}Bi_{0.1})MnO_3$ are roughly half an order of magnitude larger than those of the mixed oxide $In_2O_2 \cdot SnO_3$ which we have already reported as a novel thermoelectric oxide material (17). Moreover, the Z values presented here appear to be comparable to those of some nonoxide candidates, i.e., larger than those of B_4C, even at 1000°C, and also larger than that of β-SiC in the low and intermediate temperature regions (37). By optimizing compositions and preparative conditions as well as efforts to reduce the κ values, further improvement of the thermoelectric performance of $(Ca_{1-x}Bi_x)MnO_3$ is likely. Also, the present oxides are considered to be advantageous because of their stability at high temperature in air.

CONCLUSIONS

Electrical transport properties of partially substituted $CaMnO_3$-based perovskite-type oxides $(Ca_{0.9}M_{0.1})MnO_3$, where tri- or tetravalent elements M are Y, La, Ce, Sm, In, Sn, Sb, Pb, and Bi, were investigated in terms of a new material for high-temperature thermoelectirc conversion. Substitution for 10 at.% of the Ca site caused marked increases in the electrical conductivity σ and moderate decreases in the absolute value of the Seebeck coefficient S. This tendency can be attributed at least partly to an increase in the carrier concentration caused by the doping effect of the higher valence cations. The temperature dependence of σ showed a linear relation in plots of log σT versus $1/T$. The σ values of the substituted samples at room temperature increased with increasing ionic radii of the cation substituents, implying an increase in the mobility due to larger intersite distances for hopping. These results strongly suggest that the hopping conduction mechanism is operative in these oxides. The Bi-substituted sample showed the highest σ and fairly large S with a linear increase with temperature up to 900°C, and thereby exhibited a marked improvement in the power factor for thermoelectric conversion. Since the thermal conductivity of $(Ca_{0.9}Bi_{0.1})MnO_3$ was found to be as low as 3.8 W/mK up to 1000°C, the oxide attained a figure of merit of 0.7–0.75 $\times$ 10^{-4} K^{-1} over a wide range of temperatures (600–900°C), and the maximum ZT value was 0.085 at 900°C. The Z values obtained were comparable to those of typical nonoxide candidates for high-temperature thermoelectric materials such as B_4C and β-SiC. The good thermoelectric performance as well as excellent high-temperature durability of the metal oxides presented here suggest that small polaron oxides are of interest as potential materials for high-temperature thermoelectrics.

ACKNOWLEDGMENTS

The authors thank Mr. Yasuhiro Yamada of the Government Industrial Research Institute, Kyushu, for his kind cooperation of the laser flash measurement of κ. One of the authors (M.O.) is grateful to the Izumi Science and Technology Foundation for their financial support of part of this work.

REFERENCES

1. A. F. Ioffe, "Semiconductor Thermoelements and Thermoelectric Cooling." Infosearch, London, 1957.
2. C. Wood, *Rep. Prog. Phys.* **51,** 459 (1988).
3. C. B. Vining, "Proceedings, 12th International Conference on Ther-

moelectrics" (K. Matsuura, Ed.), p. 126. Inst. Electrical Engineers Jpn., Tokyo, 1994.
4. C. M. Bhandari and D. M. Rowe, *Contemp. Phys.* **21,** 219 (1980).
5. C. B. Vining, *J. Appl. Phys.* **69,** 331 (1991).
6. G. A. Slack and M. A. Hussain, *J. Appl. Phys.* **70,** 2694 (1991).
7. J. C. Bass and N. B. Elsner, "Proc. 3rd Int. Conf. Therm. Energ. Conv.," (K. R. Rao, Ed.) p. 8. University of Texas at Arlington, Arlington, 1980.
8. J. F. Nakahara, T. Takeshita, M. J. Tschetter, B. J. Beaudry, and K. A. Gschneidner, Jr., *J. Appl. Phys.* **63,** 2331 (1988).
9. I. Nishida, *Phys. Rev. B* **7,** 2710 (1973).
10. I. Nishida and T. Sakata, *J. Phys. Chem. Solid* **39,** 499 (1978).
11. T. Kojima, *Phys. Status Solidi (a)* **111,** 233 (1989).
12. C. Wood and D. Emin, *Phys. Rev. B* **29,** 4582 (1984).
13. M. Bouchacourt and F. Thevenot, *J. Mater. Sci.* **20,** 1237 (1985).
14. S. Yugo, T. Sato, and T. Kimura, *Appl. Phys. Lett.* **46,** 842 (1985).
15. C. G. Fonstad and R. H. Rediker, *J. Appl. Phys.* **42,** 2911 (1971).
16. T. P. Pearsall and C. A. Lee, *Phys. Rev. B* **10,** 2190 (1974).
17. M. Ohtaki, D. Ogura, K. Eguchi, and H. Arai, *J. Mater. Chem.* **4,** 653 (1994).
18. J. G. Goodenough, "Progress in Solid State Chemistry," (H. Reiss, Ed.), Vol. 5, p. 145. Pergamon, London, 1971.
19. W. J. Weber, C. W. Griffin, and J. L. Bates, *J. Am. Ceram. Soc.* **70,** 265 (1987).
20. W. J. Macklin and P. T. Moseley, *Mater. Sci. Eng. B* **7,** 111 (1990).
21. T. O. Mason, *Mater. Sci. Eng. B* **10,** 257 (1991).
22. W. J. Macklin and P. T. Moseley, *Mater. Sci. Eng. B* **10,** 260 (1991).
23. T. Kobayashi, H. Takizawa, T. Endo, T. Sato, H. Taguchi, and M. Nagao, *J. Solid State Chem.* **92,** 116 (1991).
24. G. H. Jonker and J. H. van Santen, *Physica* **16,** 337 (1950).
25. E. O. Wollan and W. C. Koehler, *Phys. Rev.* **100,** 545 (1955).
26. J. G. Goodenough, *Phys. Rev.* **100,** 564 (1955).
27. J. B. McChesney, H. J. Williams, J. F. Potter, and R. C. Sherwood, *Phys. Rev.* **164,** 779 (1967).
28. J. B. Goodenough, *J. Appl. Phys.* **37,** 1415 (1966).
29. D. P. Karim and A. T. Aldred, *Phys. Rev. B* **20,** 2255 (1979).
30. J. H. Kuo, H. U. Anderson, and D. M. Sparlin, *J. Solid State Chem.* **87,** 55 (1990).
31. H. L. Tuller and A. S. Nowick, *J. Phys. Chem. Solids* **38,** 859 (1977).
32. R. D. Shannon, *Acta Crystallogr. Sect. A* **32,** 751 (1976).
33. D. Emin, *Phys. Rev. Lett.* **35,** 882 (1975).
34. G. A. Samara, D. Emin, and C. Wood, *Phys. Rev. B* **32,** 2315 (1985).
35. R. P. Chasmar and R. J. Stratton, *J. Electron. Control* **7,** 52 (1959).
36. R. Simon, *J. Appl. Phys.* **33,** 1830 (1962).
37. K. Koumoto, C.-H. Pai, S. Takeda, and H. Yanagida, "Proceedings, 8th International Conference on Thermelectrics" (H. Scherrer and S. Scherrer, Ed.), p. 107. Inst. Natl. Polytech. Lorraine, Lorraine, 1989.